Effectiveness of implicit methods for stiff stochastic differential equations

Tiejun Li[*,1], Assyr Abdulle[2] and Weinan E[3]

[1]*LMAM and School of Mathematical Sciences, Peking University, Beijing 100871, China.*
[2]*School of Mathematics, University of Edinburgh, UK.*
[3]*Department of Mathematics and PACM, Princeton University, Princeton, NJ 08544, USA*

Abstract

In this paper we study the behavior of a family of implicit numerical methods applied to stochastic differential equations with multiple time scales. We show by a combination of analytical arguments and numerical examples that implicit methods in general fail to capture the effective dynamics at the slow time scale. This is due to the fact that such implicit methods cannot correctly capture non-Dirac invariant distributions when the time step size is much larger than the relaxation time of the system.

Keywords: implicit methods, stiff ODE, stiff SDE, invariant distribution, multiscale.

1 Introduction

Implicit stiff ODE solvers have been very successful and have become the method of choice for a large class of stiff ODEs [7]. In a system for which different components evolve on different time scales, these methods allow us to capture the dynamics of the system on the slow time scale without resolving the transient effects on the fast time scale.

Most problems for which stiff ODE solvers have been successful are those for which the trajectories reach a stable manifold after a possible initial transient corresponding to a fast scale. A convenient way to think about these problems is to use the concept of slow manifolds to which the fast variables are attracted. This happens over a short relaxation time scale over which the slow variables can be considered fixed.

---

[*]*Email: tieli@pku.edu.cn*

In this paper we examine the situation when such stiff ODE solvers are applied to stochastic dynamical systems with multiple time scales. We will demonstrate that for such systems, stiff ODE solvers may not be effective and produce wrong solutions when the fast scale dynamics are not resolved.
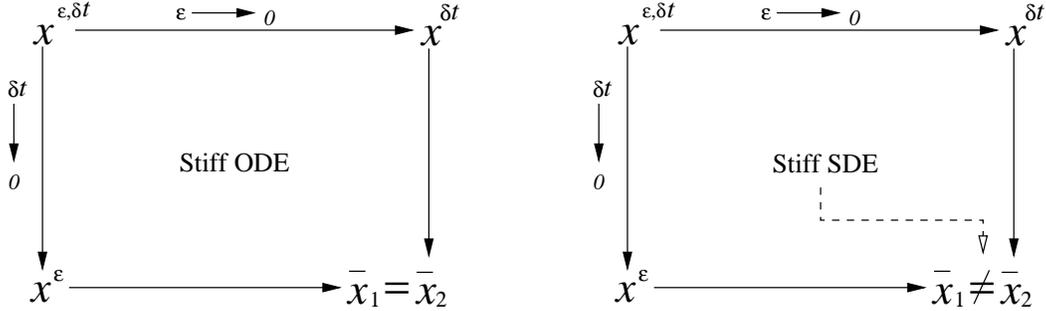

Figure 1: Illustration of the difference between implicit stiff ODE solvers applied to stiff ODEs (left) and SDEs (right).

The main point of this paper is shown in Figure 1. Denote by $x^{\varepsilon,\delta t}$ the numerical solution using an stiff ODE solver with time stepsize δt. ε is a parameter that measures the ratio of the fast and slow time scales in the system. In the case of stiff ODEs of dissipative type, we expect the following to hold:

$$\lim_{\varepsilon\to 0}\lim_{\delta t\to 0} x^{\varepsilon,\delta t} = \lim_{\delta t\to 0}\lim_{\varepsilon\to 0} x^{\varepsilon,\delta t} \tag{1.1}$$

The right hand side is much less costly to compute and this is at the heart of the effectiveness of these stiff ODE solvers. However, we will demonstrate that for stiff stochastic differential equations (SDEs) in general

$$\lim_{\varepsilon\to 0}\lim_{\delta t\to 0} x^{\varepsilon,\delta t} \neq \lim_{\delta t\to 0}\lim_{\varepsilon\to 0} x^{\varepsilon,\delta t} \tag{1.2}$$

More precisely, we will see that if we fix the ratio $\delta t/\varepsilon = c$ and we let ε go to zero, we have

$$\lim_{\delta t/\varepsilon=c,\ \varepsilon\to 0} x^{\varepsilon,\delta t} = \bar{x}^c, \tag{1.3}$$

and $\bar{x}^c$ in general varies with c.

2 An illustrative example

Consider the following example of a multiscale ODE:

$$\dot{x} = -y^2 + 5\sin(2\pi t), \tag{2.1}$$

$$\dot{y} = \frac{1}{\varepsilon}(x - y), \tag{2.2}$$

where $\varepsilon \ll 1$. In this system x is the slow variable, y is the fast variable and we are only interested in the detailed dynamics of x but not of y. Using asymptotic analysis, we see that when ε is small, y lies near the slow manifold of the system:

$$\mathcal{M} = \left\{ (x, y) \in \mathbb{R}^2, \text{ such that } y = x \right\}, \tag{2.3}$$

In fact, if y is placed away from this slow manifold, in $O(\varepsilon)$ time, the dynamics of (2.1)-(2.2) will bring y to the neighborhood of the slow manifold without causing much change to x. In other words, the quasi-equilibrium distribution obtained by holding x fixed is simply a Dirac distribution $\delta(y - y(x))$ where $y(x)$ is chosen such that $(x, y(x)) \in \mathcal{M}$. The effective dynamics of x is described by

$$\dot{\bar{x}} = -\bar{x}^2 + 5\sin(2\pi t). \tag{2.4}$$

as ε goes to zero.

Now we apply the implicit Euler scheme to this system. The setup is as follows. We take $\varepsilon = 10^{-4}$ and 10^{-6} and initial value $(x(0), y(0)) = (2, 1)$. We take the stepsize to be $\delta t = 10^{-3}, 10^{-5}$ and $\delta t = 10^{-7}$, corresponding respectively to the under-resolved and resolved case for the fast variable y. The numerical results are shown in Figure 2. We see that whether the fast dynamics is resolved or not, the correct effective behavior for the slow variable x is produced. The right panel of Figure 2 shows a brief transient period for (x, y) and afterwards the solution stays near the slow manifold $y = x$. This behavior is well known and the development of efficient solvers for such problems has been thoroughly investigated [7].

It is natural to ask whether stiff ODE solvers such as implicit Euler or the trapezoidal rule are also effective for stochastic dynamical systems that have both slow and fast time scales. We will see that the answer to this question is negative in general for implicit solvers, because the quasi-equilibrium distributions for the fast variables (with the slow variables held fixed) are not Dirac distributions. The existence of slow manifolds in the form of (2.3) is crucial for the effectiveness of the implicit methods.

To see this, let us first consider modification of the previous system by adding a noise term:

$$\dot{x} = -y^2 + 5\sin(2\pi t), \tag{2.5}$$

$$\dot{y} = \frac{1}{\varepsilon}(x - y) + \sqrt{\frac{2}{\varepsilon}} \, \dot{w}, \tag{2.6}$$

where $\dot{w}$ is the temporal Gaussian white noise which satisfies $\langle \dot{w}(t) \rangle = 0$, $\langle \dot{w}(t)\dot{w}(s) \rangle = \delta(t - s)$. Here $\langle \cdot \rangle$ means the mathematical expectation for random variables.

The noise is scaled in such a way that in the limit as $\varepsilon \to 0$, it has a finite contribution to the effective dynamics [11, 12]. The effective dynamic equations for the slow variable x
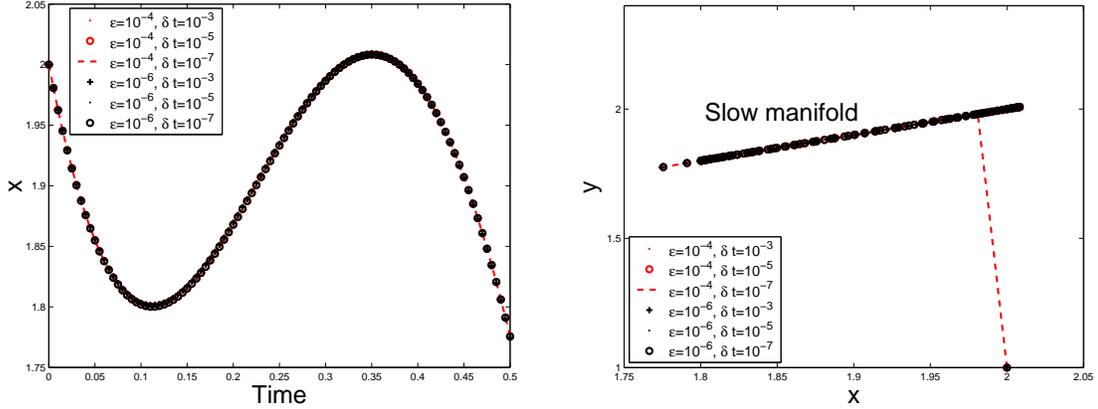
Figure 2: Implicit Euler scheme applied to equations (2.1)-(2.2). The small parameter ε is chosen as 10^{-4} and 10^{-6}, respectively. The stepsizes are $\delta t = 10^{-3}, 10^{-5}$ and 10^{-7}. The left figure shows the time history of x. The right figure shows the orbit of the numerical solution (x_n, y_n) in the x-y plane. The results shows good accuracy for x no matter whether y is resolved or not.

in the limit as $\varepsilon \to 0$ can be easily obtained using classical averaging methods and is given by

$$\dot{\bar{x}} = -\int_{\mathbb{R}} y^2 d\mu_{\bar{x}}(y) + 5\sin(2\pi t). \tag{2.7}$$

The equilibrium distribution $\mu_{\bar{x}}(y)$ is the distribution of the y variable obtained by fixing the slow variable x in (2.6) a as $\varepsilon \to 0$ and is given by

$$d\mu_{\bar{x}}(y) = \frac{1}{Z}\exp(-V(y;\bar{x}))dy, \tag{2.8}$$

where $V(y;\bar{x}) = \frac{1}{2}(y-\bar{x})^2$ and Z is a normalization constant. This distribution for y is a Gaussian $N(\bar{x}, 1)$. This gives the following effective equation for the slow variable

$$\dot{\bar{x}} = -\bar{x}^2 - 1 + 5\sin(2\pi t). \tag{2.9}$$

Next we apply the implicit Euler scheme to this problem. We use the same set of numerical parameters as before except for the time stepsize. Numerical results for this example are shown in Figure 3. We find that when $\delta t = 10^{-7}$ which is much smaller than ε, the correct effective behavior is captured. But when δt is larger than ε, the numerical solution deviates from the exact solution by a finite amount. In fact, in this case, the numerical solution gives almost the same result as the case without noise, which is incorrect. To further confirm this result, we consider the case when the ratio between δt and ε is fixed
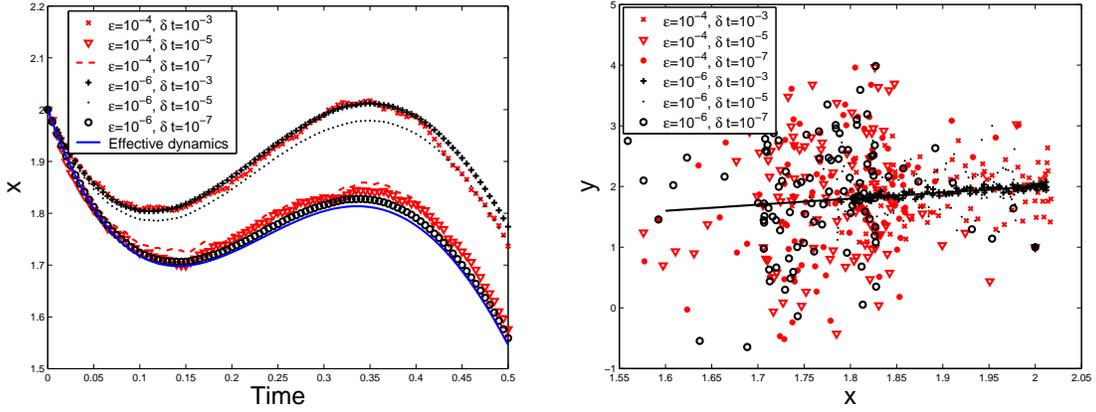
4

Figure 3: Implicit Euler scheme applied to equations (2.5)-(2.6). Here ε is chosen as 10^{-4} and 10^{-6}. The time stepsizes are chosen as $\delta t = 10^{-3}, 10^{-5}$ and 10^{-7}. The solid line in the left figure corresponds to the solution of (2.9). The left figure shows the time history of x. The right figure shows the orbit of (x_n, y_n) in the x-y plane. There is a clear gap between the under-resolved result and the resolved result. In the under-resolved case, the effect of the noise is not captured.

as 10 and 10^3, and take $\varepsilon = 10^{-6}, 10^{-7}$ and 10^{-8}. The results are shown in Figure 4. It is observed that there is a nontrivial limit as $\varepsilon \to 0$ with fixed $\delta t/\varepsilon$ and the limit is not the same as the correct effective dynamics for x.

3 Computing the equilibrium distributions

The origin of the behavior observed in the last section lies in the fact that the quasi-equilibrium distributions for the fast variables are not computed correctly. The quasi-equilibrium distributions are the invariant distributions of the fast variables when the slow variables are held fixed. They play the role of slow manifolds for SDEs. For this reason, we will conduct a careful study for the computation of the invariant distributions (for the fast variables).

3.1 Linear case

First consider a linear stochastic ODEs obtained by rescaling the harmonic oscillator in a random field:

$$\dot{y} = -\frac{1}{\varepsilon}y + \sqrt{\frac{2}{\varepsilon}}\dot{w}, \quad y(0) = y_0, \quad 0 < \varepsilon \ll 1. \tag{3.1}$$
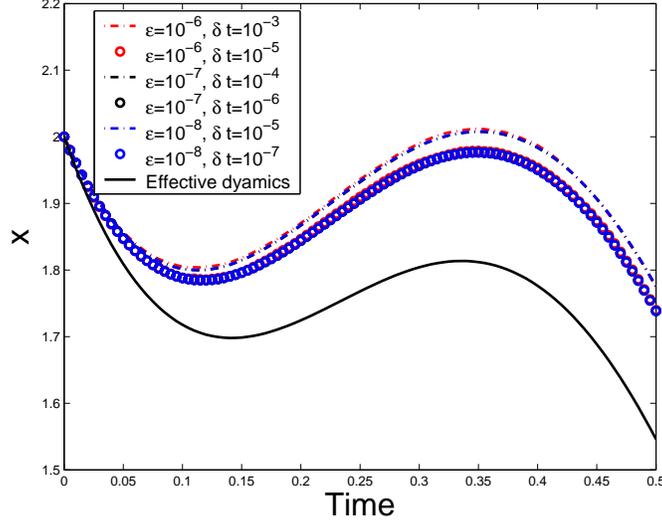
Figure 4: Implicit Euler scheme applied to equations (2.5)-(2.6) with fixed $\delta t/\varepsilon = 10$ (dashdots) and 10^3 (circles) when $\varepsilon = 10^{-6}, 10^{-7}$ and 10^{-8}. Two nontrivial limits are obtained numerically. The solid line is the correct effective dynamics.

y is an Ornstein-Uhlenbeck process with exact solution

$$y(t) = \exp\left(-\frac{t}{\varepsilon}\right)y_0 + \int_0^t \sqrt{\frac{2}{\varepsilon}} \exp\left(-\frac{t-s}{\varepsilon}\right)dw_s. \tag{3.2}$$

From the explicit solution (3.2), one sees that the y is a Gaussian stochastic process (if y_0 is normally distributed or constant) and converges to the Gaussian invariant measure $N(0,1)$ as $t \to \infty$.

Consider now the stochastic $\theta-$method

$$y_{n+1} = y_n + (1-\theta)\delta t f(y_n) + \theta \delta t f(y_{n+1}) + (\delta t)^{\frac{1}{2}} g(y_n)\delta w_n, \tag{3.3}$$

where δw_n are independently and identically distributed (i.i.d.) Gaussian random variable $N(0,1)$ and where $f(y(t)) = -\frac{1}{\varepsilon}y$ and $g(y(t)) = \sqrt{\frac{2}{\varepsilon}}$ for the SDE (3.2). The process (3.3) defines a family of numerical methods and for $\theta = 0$ we obtain the well-known Euler Maruyama method, for $\theta = 1/2$ the trapezoidal rule and for $\theta = 1$ the Euler implicit method. For the problem (3.2), the method (3.3) can be rewritten as

$$y_{n+1} = \frac{1}{1+(\delta t/\varepsilon)\theta}\left((1-(\delta t/\varepsilon))(1-\theta)y_n + \sqrt{2(\delta t/\varepsilon)}\delta w_n\right) = r_\theta(\delta t/\varepsilon)y_n + s_\theta(\delta t/\varepsilon)\delta w_n. \tag{3.4}$$

6

The invariant distribution of the discrete system is also Gaussian. Computing the mean

$$\mathbb{E}(y_{n+1}) = r_\theta(\delta t/\varepsilon)\mathbb{E}(y_n), \tag{3.5}$$

on easily find that for $y_0 \neq 0$, $\lim_{n\to\infty} \mathbb{E}(y_n) = 0$ if an only if $|r_\theta(\delta t/\varepsilon)| \leq 1$, which holds for any time step δt if an only if $1/2 \leq \theta \leq 1$. This is well known from the theory for deterministic ODEs and is related to the so-called $A-$stability of the $\theta-$method for $1/2 \leq \theta \leq 1$ ([7],[9]). For the second moment, assuming $1/2 \leq \theta \leq 1$ on find for any time step δt that

$$\lim_{n\to\infty} \mathbb{E}(|y_n|^2) = \mathbb{E}(|y_\infty|^2) = \frac{1}{1 - (1 - 2\theta)\frac{\delta t}{2\varepsilon}}. \tag{3.6}$$

Thus

$$\lim_{\delta t\to 0}\lim_{\varepsilon\to 0} \mathbb{E}(|y_\infty|^2) = \lim_{\varepsilon\to 0}\lim_{\delta t\to 0} \mathbb{E}(|y_\infty|^2) \tag{3.7}$$

if and only if $\theta = 1/2$. We see that that for the Euler implicit method ($\theta = 1$) when $\delta t/\varepsilon$ is large, the computed variance is much smaller than the correct value. And as $\delta t/\varepsilon \to \infty$, the variance tends to zero! Similar behavior can be observed for $1/2 < \theta \leq 1$. This is a consequence of the fact that for a fixed ration $\delta t/\varepsilon = c$, $\lim_{c\to\infty} |r_\theta(\delta t/\varepsilon)| = 0$. This property, known as $L-$stability in the theory for deterministic ODEs is suitable for stiff ODEs, since it damps the oscillaions of the iteration (3.4). This damping in the stochastic case prevents the correct computation of the numerical variance. This is the case observed in Figure 3, i.e. the effect of the fluctuations is not captured.

These results can be used to explain the phenomena observed in the previous section. Given $\delta t/\varepsilon = c$ and $x = \bar{x}^c$, denote by $\mu^c_{\bar{x}^c}(y)$ the computed numerical invariant distribution for the fast variable y as $\varepsilon \to 0$, then for small values of δt, the effective dynamics for the numerical solution of the slow variable, denoted by $\bar{x}^c$, is given approximately by

$$\dot{\bar{x}}^c = -\int_R y^2 d\mu^c_{\bar{x}^c}(y) + 5\sin(2\pi t). \tag{3.8}$$

Since μ^c is in general different from the correct quasi-equilibrium distribution μ and in particular the variances of y are not the same for these distributions, we expect to get incorrect numerical results for the slow dynamics.

However, if one uses the trapezoidal rule $\theta = 1/2$ we see from (3.6) that its invariant distribution is also Gaussian with mean 0 and variance 1, which is the desired result. These phenomena are the same as the ones observed in [1] for tau-leaping methods for jump processes. From this we expect that when the trapezoidal rule is applied to the example discussed earlier, accurate numerical solution will be obtained even if the fast dynamics is not well-resolved. Figure 5 confirms this. However, this property of the trapezoidal rule is not generic — it is the consequence of the linearity of the system as illustrated in the next section.
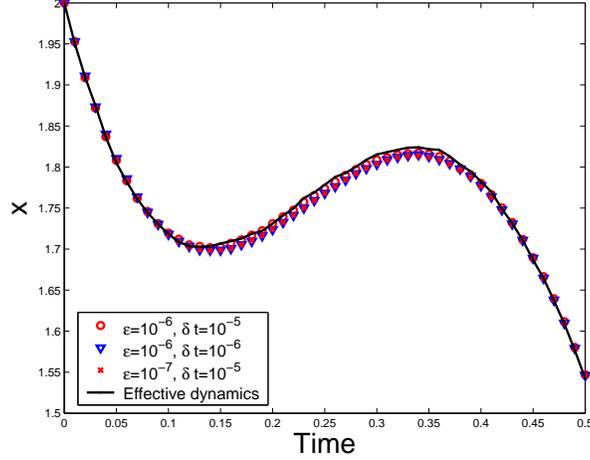
Figure 5: Trapezoidal rule applied to equations (2.1)-(2.2). The ratio $\delta t/\varepsilon$ is chosen from $10^2, 10$ to 1. The small parameter ε is chosen as 10^{-6} or 10^{-7}. The solid line is the correct effective dynamics.

3.2   Nonlinear case

Let us consider a nonlinear example

$$\dot{y} = -\frac{1}{\varepsilon}V'(y) + \sqrt{\frac{2}{\varepsilon}}\dot{w}, \quad y(0) = y_0, \quad 0 < \varepsilon \ll 1. \tag{3.9}$$

It is well-known that the equilibrium distribution of y is the Gibbs measure

$$\frac{1}{Z}\exp(-V(y)), \tag{3.10}$$

where $Z = \int \exp(-V(y))dy$ is a normalization constant. We will investigate two cases.

- Symmetric potential
$$V(y) = (y^2 - 1)^2, \tag{3.11}$$

- Asymmetric potential
$$V(y) = (y^2 - 1)^2 - 0.5y. \tag{3.12}$$

Let us first consider the implicit Euler scheme and trapezoidal scheme applied to the symmetric potential case. We fix $\varepsilon = 10^{-3}$, and choose δt from $10^{-2}, 10^{-3}, 10^{-4}, 10^{-5}$ to 10^{-6}. It is straightforward to see that the numerical results depend on the ratio $\delta t/\varepsilon$, we actually obtain results for the case when $\delta t/\varepsilon$ takes the values $10^{-3}, 10^{-2}, 10^{-1}, 10$. We obtain the limit distribution with 20000 samples from a deterministic initial condition $y_0 = -2$.

8

To plot the probability density function (pdf), we make statistics for the sample data in an equi-subdivided interval. In the i-th bin the number of the points, say n_i, is counted, then the pdf value in the center of this bin will be $n_i/(Nh)$, where N is the total number of points, and h is the bin size. Figure 6 summarizes our findings. We see that for both the implicit Euler scheme and the trapezoidal rule, the numerical invariant distribution is accurate only when the ratio $\delta t/\varepsilon$ is small, and large discrepancies are found otherwise.
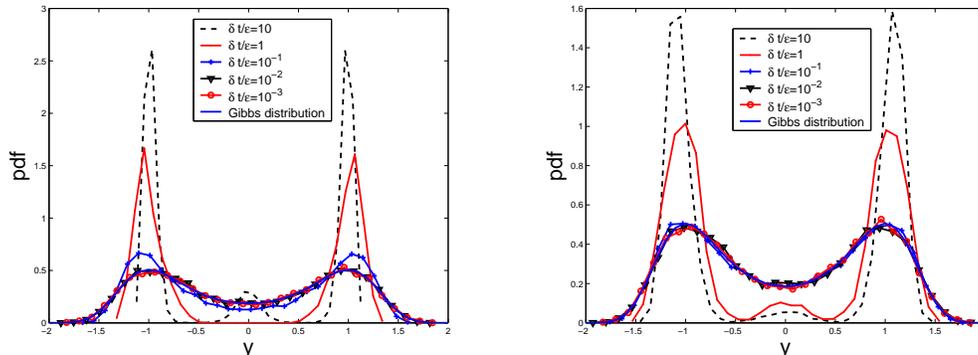

Figure 6: Invariant distribution computed using the implicit Euler scheme (left) and trapezoidal rule (right) for the case of symmetric double-well potential. $\varepsilon = 10^{-3}$. The time stepsize $\delta t = 10^{-2}, 10^{-3}, 10^{-4}, 10^{-5}$ and 10^{-6}. Sample size is 20000.

From Figure 6 we also see that when $\delta t/\varepsilon$ is large, the distribution becomes more and more atomic. An asymptotic analysis shows that in the limit when $\mu = \varepsilon/\delta t \to 0$, we have

$$y_n \approx y^* + \frac{\sqrt{2\mu}}{V''(y^*)}\delta w_n + \cdots , \tag{3.13}$$

where y^* is one of the local minima for the potential $V(y)$.

Similar results are obtained for the case when the potential is asymmetric. The results are summarized in Figure 7. Same numerical parameters are used.

This result suggests that for nonlinear systems, the behavior of implicit Euler and the trapezoidal rule is similar, when applied to SDEs with multiple time scales and the fast dynamics are not well-resolved. In other words, in general one should not expect the trapezoidal rule to capture the slow dynamics correctly if the fast dynamics is not resolved. To see that this is actually the case, let us consider the SDE

$$\dot{x} = -2e^y + 5\sin(2\pi t), \tag{3.14}$$

$$\dot{y} = \frac{1}{\varepsilon}(x - V'(y)) + \sqrt{\frac{2}{\varepsilon}}\,\dot{W}, \tag{3.15}$$
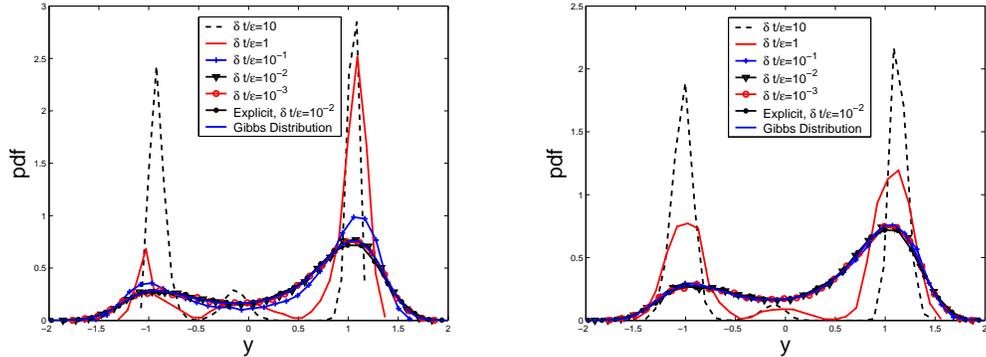
9

Figure 7: Invariant distributions computed using the implicit Euler scheme and the trapezoidal rule for the case of asymmetric double-well potential. $\varepsilon = 10^{-3}$. The time stepsize $\delta t = 10^{-2}, 10^{-3}, 10^{-4}, 10^{-5}$ and 10^{-6}. Sample size is 20000.

where $V(y) = (y^2 - 1)^2 - 0.5y$, and $\varepsilon = 10^{-4}$. We apply the trapezoidal rule to this system. The initial state is $(x_0, y_0) = (0, 1)$. The time stepsizes are taken as $\delta t = 10^{-3}, 10^{-4}, 10^{-5}$ and 10^{-6}. The numerical results are shown in Figure 8. We see clearly that the under-resolved results are quite different from the resolved ones. The right figure in Figure 8 shows that the orbits of (x_n, y_n) cluster around the slow manifold in the case without noise.

To further clarify the situation, we study the case when keeping $\delta t / \varepsilon$ constant but letting ε go to zero. The results are shown in Figure 9. We see also that the limits seem to exist, but they are different from the correct value.

4   Conclusion

Implicit stiff ODE solvers are well-accepted schemes for solving stiff ODEs such as the ones that arise from modeling chemical kinetics. Their effectiveness, however, seems to rely on the existence of slow manifolds in a traditional sense, as in (2.3) for the system (2.1)-(2.2). In the stochastic setting they can also be efficient for asymptotically mean square problems [10]. For the examples considered in this paper, we may think of slow manifolds in a generalized sense. For example, for the SDEs considered in Sections 2 and 3, there are indeed slow manifolds for the fast variable in the space of probability distributions, which are the quasi-equilibrium distributions $\mu_{\bar{x}}(y)$. However, we have demonstrated that from a numerical viewpoint, there is an essential difference between these two cases, and traditional implicit stiff ODE solvers are not effective if the slow manifolds only exist in the generalized sense. For these reasons, explicit methods of the type discussed in [2-6,13] are of particular interest for such systems.
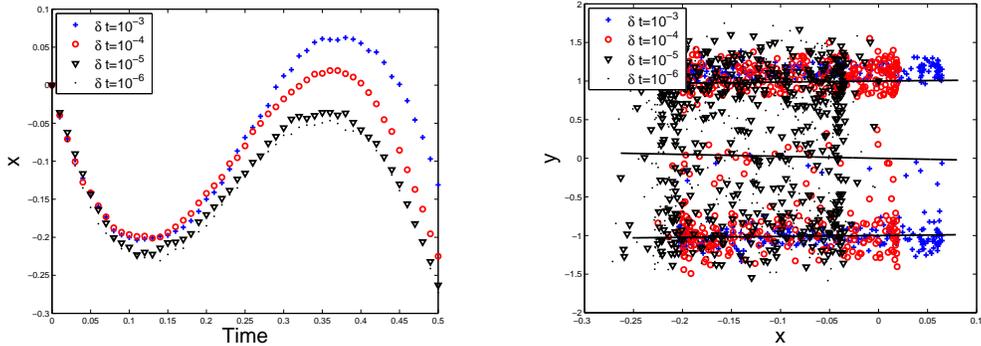
Figure 8: The trapezoidal rule applied to system (3.14)-(3.15). $\varepsilon = 10^{-4}$. The time stepsize $\delta t = 10^{-3}$ (plus), 10^{-4} (circles), 10^{-5} (triangle down), and 10^{-6} (dots). The solid curve in the right figure is the slow manifold without noise. It can be observed that when δt is smaller, more points fall between the upper and lower solid lines instead of concentrating around these two lines. This can be explained from the results obtained in Figure 7.

Acknowledgement

References

[1] Y. Cao, L. Petzold, M. Rathinam and D.T. Gillespie, The numerical stability of leaping methods for stochastic simulation of chemically reacting systems, J. Chem. Phys. 121 (2004), 12169-12178.

[2] W. E, Analysis of the heterogeneous multiscale method for ordinary differential equations, Comm. Math. Sci. 1 (2003), 423-436.

[3] W. E and B. Engquist, The heterogeneous multiscale methods, Comm. Math. Sci. 1 (2003), 87-132.

[4] W. E, B. Engquist, X. Li, W. Ren and E. Vanden-Eijnden, Heterogeneous multiscale methods: A review, Commun. Comput. Phys., 2 (2007), 367-450.
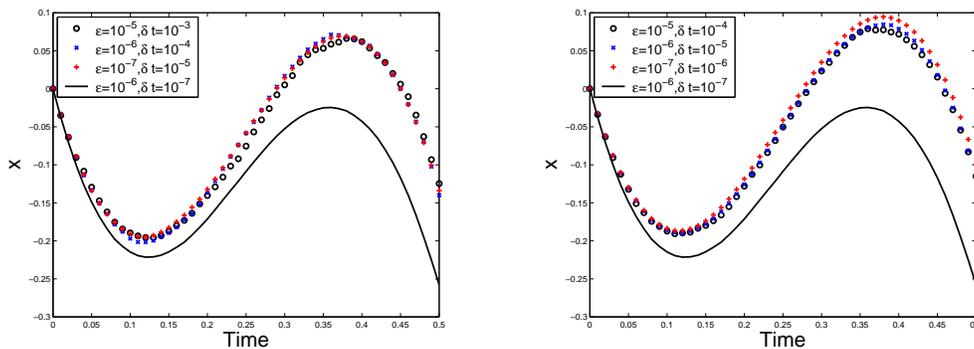
Figure 9: Trapezoidal rule applied to system (3.14)-(3.15). The ratio $\delta t/\varepsilon$ is kept as 10^2 in the left figure, and 10 in the right figure. $\varepsilon = 10^{-5}, 10^{-6}$ and 10^{-7}. The solid curve in both figures corresponds to $\varepsilon = 10^{-6}, \delta t = 10^{-7}$.

[5] W. E, D. Liu and E. Vanden-Eijnden, Analysis of multiscale methods for stochastic differential equations, Comm. Pure Appl. Math. 58 (2005), 1544-1585.

[6] B. Engquist and R. Tsai, Heterogeneous multiscale methods for stiff ODEs, Math. Comp. 74 (2005), 1707-1742.

[7] E. Hairer and G. Wanner, Solving ODEs: Stiff and Differential-Algebraic Problems, Vol. II, Springer-Verlag, Berlin and Heidelberg, 1996, Second Edition.

[8] E. Hairer, C. Lubich and G. Wanner, Geometric numerical integration: structure-preserving algorithms for ordinary differential equations, Springer Verlag, Berlin and New York, 2002.

[9] D.J. Higham, Mean-square and asymptotic stability of numerical methods for stochastic ordinary differential equations, SIAM J. Numer Anal., 38 (2000), 753-769.

[10] P.E. Kloeden and E. Platen, Numerical Solution of Stochastic differential equations, Springer-Verlag, Berlin and Heidelberg, 1992.

[11] T.G. Kurtz, A limt theorem for perturbed operator operator semigroups with applications to random evolutions, J. Funct. Anal. 12 (1973), 55-67.

[12] G.C. Papanicolaou, Introduction to the asymptotic analysis of stochastic equations, Lectures in Applied Mathematics, Vol. 16, 109-147, American Mathematical Society, Providence, Rode Island, 1977.

[13] E. Vanden-Eijnden, Numerical techniques for multi-scale dynamical systems with stochastic effect, Comm. Math. Sci. 1 (2003), 385-391.